Toxicology 395 (2018) 15–22

Contents lists available at ScienceDirect

Toxicology

journal homepage: www.elsevier.com/locate/toxicol

PFE-360-induced LRRK2 inhibition induces reversible, non-adverse renal changes in rats

Michael Aagaard Andersen[a,b,*], Karen Malene Wegener[c], Steen Larsen[c], Lassina Badolo[d], Garrick Paul Smith[e], Ross Jeggo[a], Poul Henning Jensen[b], Florence Sotty[a], Kenneth Vielsted Christensen[a], Annemette Thougaard[f]

[a] Department of Neurodegeneration, Neuroscience Drug Discovery DK, H. Lundbeck A/S, Valby, Denmark
[b] Department of Biomedicine, Dandrite, Faculty of Health, Aarhus University, Aarhus, Denmark
[c] Department of Regulatory Toxicology & Safety Assessment, H. Lundbeck A/S, Valby, Denmark
[d] Department of Discovery DMPK, H. Lundbeck A/S, Valby, Denmark
[e] Department of Discovery Chemistry 2, H. Lundbeck A/S, Valby, Denmark
[f] Department of Exploratory Toxicology, Nonclinical Safety Research, H. Lundbeck A/S, Valby, Denmark

ABSTRACT

Parkinson's disease (PD) is a progressive neurodegenerative disorder for which there is no existing therapeutic approach to delay or stop progression. Genetic, biochemical and pre-clinical studies have provided evidence that leucine-rich-repeat-kinase-2 (LRRK2) kinase is involved in the pathogenesis of PD, and small molecule LRRK2 inhibitors represent a novel potential therapeutic approach. However, potentially adverse target-related effects have been discovered in the lung and kidneys of LRRK2 knock-out (ko) mice and rats. It is unclear if the LRRK2 ko effect in the kidneys and lung is also induced by pharmacological inhibition of the LRRK2 kinase. Here, we show that treatment with the LRRK2 inhibitor PFE-360 in rats induces a morphological kidney phenotype resembling that of the LRRK2 ko rats, whereas no effects were observed in the lung. The PFE-360 treatment induced morphological changes characterised by darkened kidneys and progressive accumulation of hyaline droplets in the renal proximal tubular epithelium. However, no histopathological evidence of renal tubular injury or changes in the blood and urine parameters that would be indicative of kidney toxicity or impaired kidney function were observed after up to 12 weeks of treatment. Morphological changes were detected in the kidney after 2 weeks of treatment and were partially reversible within a 30 day treatment-free period. Our findings suggest that pharmacological LRRK2 inhibition may not have adverse consequences for kidney function.

1. Introduction

Missense mutations in leucine-rich repeat kinase 2 (LRRK2) are the most common genetic cause of late onset Parkinson's disease (PD). LRRK2 is a multi-domain protein and mutations in many of these domains increase the risk of PD (Zimprich et al., 2004a, 2004b). The G2019S mutation is the most prevalent and is located in the kinase domain, resulting in increased kinase activity. Mutations in the Roc-COR and WD40 domain outside of the kinase domain have a similar effect on kinase activity (Reynolds et al., 2014). These observations have led to the development of LRRK2 knock-out (ko) animal models and small molecule LRRK2 kinase inhibitors (hereafter referred to as LRRK2 inhibitors) with the prospect of validating a novel disease-modifying target. However, the LRRK2 ko and D1994A-LRRK2 (kinase dead) transgenic animals have provided indications of potentially adverse effects on lung morphology as well as kidney morphology and function. The lung shows abnormal accumulation of lamellar bodies in type 2 pneumocytes and the kidneys show hyaline droplets and a lipofuscin-like brown pigment in the renal proximal tubular epithelium (Baptista et al., 2013; Herzig et al., 2011). Recent studies, using small molecule LRRK2 inhibitors, have not provided a uniform answer as to what extent lung and kidney changes emerge after pharmacological inhibition of the LRRK2 kinase. Some investigators have reported no adverse effects after 4 weeks of treatment in rats (Daher et al., 2015), whereas the lung phenotype of LRRK2 ko has been replicated within 2 weeks in mice and non-human primates dosed with LRRK2 inhibitors, including MLi-2, GNE-7915 and GNE-0877 (Fell et al., 2015; Fuji et al., 2015).

Morphological findings similar to those reported in LRRK2 ko animals were observed in the kidneys of rats treated with a LRRK2

* Corresponding author at: Department of Neurodegeneration, Neuroscience Drug Discovery DK, H. Lundbeck A/S, Valby, Denmark.
E-mail address: aaga@lundbeck.com (M.A. Andersen).

https://doi.org/10.1016/j.tox.2018.01.003
Received 23 November 2017; Received in revised form 22 December 2017; Accepted 3 January 2018
Available online 04 January 2018

inhibitor in our laboratory, thus warranting further exploration of the potential adverse effects of pharmacological LRRK2 kinase inhibition (hereafter referred to as LRRK2 inhibition). This was pursued by studying lung and kidney changes in rats dosed with the potent and selective LRRK2 inhibitor PFE-360 (Baptista et al., 2015). The progression of kidney changes was studied after 1–12 weeks of treatment, and the reversibility was investigated over a 30 day treatment-free period. Whilst no treatment-related changes were observed in the lung, we report for the first time that pharmacological LRRK2 inhibition induced morphological changes in rat kidneys that closely resemble the kidney phenotype found in LRRK2 ko rats. Furthermore, kidney changes were partially reversible within a 30 day treatment-free period.

2. Methods

2.1. Ethical statement

All experiments were carried out in accordance with the European Communities Council Directive (86/609/EEC) for the care and use of laboratory animals and the Danish legislation regulating animal experiments.

2.2. Animals

Female Sprague Dawley rats (NTac:SD) weighing 225–250 g were purchased from Taconic. The rats were group housed in controlled temperature (22 ± 1.5 °C) and humidity conditions (55–65%) and kept in a 12:12 h light/dark cycle (lights on at 06:00 h). Food and water were available *ad libitum* (pellet diet, Altromin 1324, Brogaarden Denmark). The water was acidified with HCl to pH 3.6 ± 0.5.

2.3. PFE-360 treatment

PFE-360 (Baptista et al., 2015) (Ref type: Online Source) was synthesized at H. Lundbeck as described in patent application US2014/005183 (Example 217) (1-methyl-4-(4-morpholino-7H-pyrrolo[2,3-*d*]pyrimidin-5-yl)pyrrole-2-carbonitrile) and dissolved in a vehicle consisting of 10% captisol adjusted to pH 2 with 1 M methanesulfonic acid to a final concentration of 3 mg/ml and administrated by oral gavage using plastic feeding tubes. A dose of 4 or 7.5 mg/kg *bis in die* (BID) was used, each dosing separated by 12 h. Two different batches of PFE-360 was used and the purity was determined by UV detection and evaporative light scattering detection (ELSD) (Purity of batch 1: UV: 96.65% and ELSD: 99.47%; Purity of batch 2: UV: 99.19% and ELSD: 100%).

2.4. Experimental design

Initially, kidney and lung morphology (organ weights, macroscopic and microscopic examination) as well as kidney function (urinalysis, clinical chemistry and haematology) were evaluated as part of a pharmacology study with PFE-360 given orally to rats for 10–12 weeks at 7.5 mg/kg BID (vehicle: N = 5 and PFE-360: N = 6). The bodyweights were measured weekly during the study. The plasma exposures were measured 6 h after the last dose. For a graphic overview of the study designs see Suppl. Fig. 1.

Subsequently, two repeat-dose experimental setups in rats were used to determine the time to onset and the reversibility of the morphological kidney changes. As the variation in the morphology of the kidney findings was very small between animals in the initial study, we chose, in accordance with the 3R's, to use group sizes of N = 2-4 in these experiments.

To establish the time at which morphological changes develop in the kidneys and to investigate the treatment effect on the renal LRRK2 expression, rats were dosed orally with PFE-360 at 7.5 mg/kg BID and the kidneys were examined macroscopically, microscopically and for the expression level of total LRRK2 and LRRK2-pSer935 (LRRK2 phosphorylated at serine 935) after 1, 2, 4, 6 (N = 2 per time point) and 8 (N = 3) weeks of treatment. A vehicle group treated for 8 weeks BID (N = 4) was included. The plasma exposure was measured 1 or 12 h after the last dose.

In the reversibility study, treatment was stopped after 8 weeks of oral administration of PFE-360 at 4 mg/kg BID or 7.5 mg/kg BID, and kidney morphology (macroscopic and microscopic examination) was assessed on day 2, 9, 16 and 30 after cessation of treatment (vehicle group: N = 4 (Day 2, 9 and 30) and N = 2 (Day 16), PFE-360 at 4 mg/kg group: N = 2 per time point and PFE-360 at 7.5 mg/kg group: N = 4 per time point).

In addition, the plasma exposure of PFE-360 was measured at multiple time points after a single oral dose of 4 or 7.5 mg/kg.

2.5. Blood sampling for exposure analysis

Blood samples were collected from the tail vein or terminally from the heart under deep anaesthesia for PFE-360 exposure analysis. The blood samples were taken at 0.25, 0.5, 1, 2, 4, 6, and 8 h after a single PFE-360 dose of 4 mg/kg and at 1, 3, 6 and 12 h after a single PFE-360 dose of 7.5 mg/kg. In addition, samples were collected following 1–12 weeks of treatment with 7.5 mg/kg PFE-360 BID at 1, 6 and 12 h after dosing. The blood samples were stabilised with K_3EDTA and plasma was isolated by centrifugation at 2000*g*, 4° C, for 15 mins.

2.6. Bioanalysis

Calibration standards and quantification control samples were prepared and validated according to internal protocols. Quantification of the total PFE-360 concentration in plasma was performed using a LC–MS/MS platform (Xevo TQS triple quadrupole (TQ) mass spectrometer operated in electrospray MS/MS mode (multiple reaction mode, MRM) and coupled to a Waters Acquity UPLC controlled by Mass Lynx software version 4.1). The free fraction of PFE-360 in plasma was determined as described previously (Bundgaard et al., 2012), and used to calculate the unbound PFE-360 concentration in plasma.

The unbound kidney concentrations were estimated from the unbound plasma concentrations assuming the free drug hypothesis (Trainor, 2007), i.e. that the concentrations of unbound PFE-360 in plasma equal that of kidney under the test conditions.

2.7. Urinalysis

Urine was sampled from the rats treated for 10–12 weeks by cystocentesis under deep anaesthesia before sacrifice. The urine was stored at −20 °C until analysis. Standard urinalysis (pH, protein, specific gravity, erythrocytes and glucose) was performed using Multistix®10 SG and a CLINITEK®500 Analyser. In addition, lipocalin-2, osteopontin, kidney injury marker 1 (KIM-1) and creatinine were determined in the urine using the MSD Kidney Injury Panel 1 (rat) Assay Kit (Meso Scale Discovery, Rockville, USA). All lipocalin-2, osteopontin and KIM-1 values were normalised to creatinine.

2.8. Haematology and clinical chemistry

Blood samples were collected from the rats treated for 10–12 weeks by heart puncture under deep anaesthesia prior to sacrifice. Haematology analysis of K_3EDTA stabilised blood was performed within 6 h with an Advia® 2120i Hematology Analyzer using Multispecies software assessing red blood cell parameters, haemoglobin, platelet parameters and white blood cell differential counts. In addition, serum was obtained from blood tubes with Serum Clot activator and analysed for a standard clinical chemistry panel including urea, creatinine and albumin concentrations with an ABX Pentra 400 clinical chemistry analyser.

2.9. Sacrifice and necropsy procedures

The rats were anaesthetised with an intraperitoneal injection of Avertin, 120 mg/kg, urethane, 1.6-2.1 g/kg or with Hypnorm/Dormicum (corresponding to 157 μg/kg fentanyl, 5 mg/kg fluanisone and 2.5 mg/kg midazolam). The anaesthetised rats were sacrificed by exsanguination from the heart, perfused intracardially with heparinized saline (100 ml, 0.3% heparin) and tissues were collected for organ weights, LRRK2 expression analysis, and macroscopic and microscopic evaluation. The animals used for the time to onset experiment were not perfused prior to organ harvest.

2.10. LRRK2 and LRRK2-pSer935 expression in kidney samples

The expression levels of total LRRK2 and LRRK2-pSer935 were assessed by western blot in kidney samples taken at 1 h or 12 h after dosing following 1, 2, 4, 6 and 8 weeks of treatment with vehicle or 7.5 mg/kg PFE-360 BID. As there was no difference in the renal LRRK2 inhibition (the ratio of LRRK2-pSer935/total LRRK2) between 1, 2, 4, 6 and 8 weeks of PFE-360 dosing, all the results were pooled by the 1 h or 12 h time points, respectively.

The kidney samples were homogenized using Precellys lysing kit 0.5 ml (Precellys Lysing Kit CK14 0.5 ml) in a cell lysis buffer (Sigma: C2978) with protease (1 tablet per 50 ml lysis buffer) (Roche: 11 697 498 011) and phosphatase inhibitors (1 tablet per 10 ml lysis buffer) (Roche 04 906 837 001). Samples were homogenised for 2 × 30 s at 5000 rpm using a Precellys 24 homogenizer (Bertin Technologies) and subsequently spun at 3000 g for 30 mins at 4° C. The supernatants were collected for total protein concentration measurements using a BCA assay (Thermo Scientific, Pierce™ BCA protein assay kit, #23225). Samples were diluted and supplemented with loading buffer (Invitrogen, NuPAGE, LDS sample Buffer (4×), NP0007) to reach a final protein concentration of 1 μg/μl.

LRRK2 and LRRK2-pSer935 were separated from other proteins on a 3–8% Tris-Acetate gel (NuPAGE® Tris-Acetate Mini Gels, Life Technologies). An amount of 15 μg total protein was loaded into each well. Proteins were transferred onto Immobilon-FL PVDF membranes (Millipore, Billerica, US). Membranes were incubated with primary antibodies overnight at 4° C: mouse monoclonal [N241A/34] anti-LRRK2 antibody (1:2000; NeuroMab) and rabbit monoclonal [UDD2 10(12)] anti-LRRK2-pSer935 antibody (1:1000; RabMAbs®, Abcam). The membranes were then washed and incubated with secondary antibodies for 1 h at room temperature: Goat-Anti-rabbit IgG-IRDye® 800CW antibody (1:10,000; Rockland Immunochemicals Inc.) and Goat anti-mouse IgM Alexa Fluor® 680 (1:20,000; Life Technologies). The proteins were visually detected by infrared imaging using Li-Cor Odyssey CLx (LI-COR). Membranes were scanned and band intensities were quantified using the Li-Cor Odyssey software (Image Studio version 3.1.4).

2.11. Kidney and lung histopathology

Following necropsy, the kidneys and lungs were collected and fixed in 4% v/v neutral buffered formaldehyde solution for a minimum of 48 h. The tissues were dehydrated and paraffin embedded. Sections were cut at 5 μm on a sliding microtome (Finesse™ Microtome), mounted on glass slides and stained with haematoxylin and eosin (HE). Additional kidney sections were stained by Schmorĺs method for reducing substances (Luna, 1968), a ferric ferricyanide reduction test traditionally used to demonstrate lipofuscin, and Perl's method for ferric iron/haemosiderin (Luna, 1968).

2.12. Statistical analysis

All statistical analysis and graphs were made with GraphPad Prism 7.02 and all data were checked for normal distribution. Comparison of two groups was done using a *t*-test, whilst comparison of more than two groups was done using a one-way ANOVA with Tukey's multiple comparison test.

3. Results

3.1. PFE-360 pharmacokinetics and pharmacodynamics

We observed kidney findings similar to those reported in LRRK2 ko animals in a rat pharmacology study using the potent and selective LRRK2 inhibitor PFE-360. These initial findings were pursued in additional experiments. The apparent in vivo IC_{50} of PFE-360 has previously been determined to 3 nM (Baptista et al., 2015), and was confirmed in our laboratory (data not shown). In order to achieve full peripheral LRRK2 inhibition, an estimated PFE-360 unbound plasma concentration of 10-fold the IC_{50} (~30 nM) at trough was targeted.

The PFE-360 plasma concentrations obtained 12 h after a single dose of 7.5 mg/kg showed an average unbound PFE-360 plasma concentration of 25 ± 15 nM (mean ± SEM). A single dose of 4 mg/kg PFE-360 resulted in an unbound plasma concentration of 23 ± 5 nM (mean ± SEM) 8 h after dosing. The half-life of PFE-360 was calculated to be 2.8 ± 1.3 h (mean ± SEM), and it was estimated that at trough levels, rats dosed with 4 mg/kg BID would not have full LRRK2 inhibition in peripheral organs such as the kidneys (Fig. 1A).

The unbound plasma concentrations after multiple doses of 7.5 mg/kg PFE-360 BID were lower than after a single dose of 7.5 mg/kg PFE-360 at the early timepoints 1 and 6 h (compare Fig. 1B and A), probably due to induction of metabolism. At 12 h after dosing, the concentration was 25 ± 7 nM, ensuring close to full LRRK2 inhibition at all time points when using BID dosing with 12 h interval. The multiple dose data are a combination of data from the 10–12 week and time to onset experiments (Fig. 1B).

3.2. LRRK2 and LRRK2-pSer935 renal expression after PFE-360 treatment

There was no significant change in total LRRK2 expression in the kidneys after up to 8 weeks of dosing with PFE-360 at 7.5 mg/kg BID at either 1 or 12 h after dosing compared with vehicle treated rats (one-way ANOVA; $p = 0.54$) (Fig. 1D). As expected and consistent with the PFE-360 plasma exposure results, there was no detectable LRRK2-pSer935 immunoreactivity on Western blots from animals treated with PFE360 at neither 1 h nor 12 h after dosing and the LRRK2-pSer935/total LRRK2 ratio was significantly decreased at both 1 h and 12 h after dosing (one-way ANOVA; $p < 0.001$; Tukey's multiple comparison; vehicle vs 1 h: $p = 0.0027$ and vehicle vs 12 h: $p = 0.0003$), confirming full LRRK2 inhibition at all time points after BID dosing with PFE-360 at 7.5 mg/kg (Fig. 1E).

3.3. Bodyweights, haematology, clinical chemistry and urinalysis after PFE-360 treatment for 10–12 weeks

The terminal bodyweights were not different between rats dosed BID with 7.5 mg/kg PFE-360 and vehicle (t-test; $p > 0.05$) (Suppl. Table 1), and no significant changes were found in haematology and clinical chemistry parameters after the PFE-360 treatment when compared with vehicle (t-test; $p > 0.05$. Haematology; Suppl. Table 2, clinical chemistry; Suppl. Table 3).

Due to limitations in urine sample volume, the standard urinalysis was performed in only two animals in each group of vehicle- and PFE360-treated rats, respectively. There were traces of blood in the samples, likely coming from the cystocentesis used to obtain the samples. The measured parameters pH, protein, specific gravity and glucose were similar in all animals (data not shown). None of the urine kidney markers; creatinine, KIM-1, lipocalin-2 or osteopontin, showed a significant difference between vehicle-treated rats and rats treated with PFE-360 (*t*-test; $p > 0.05$, Suppl. Table 4)

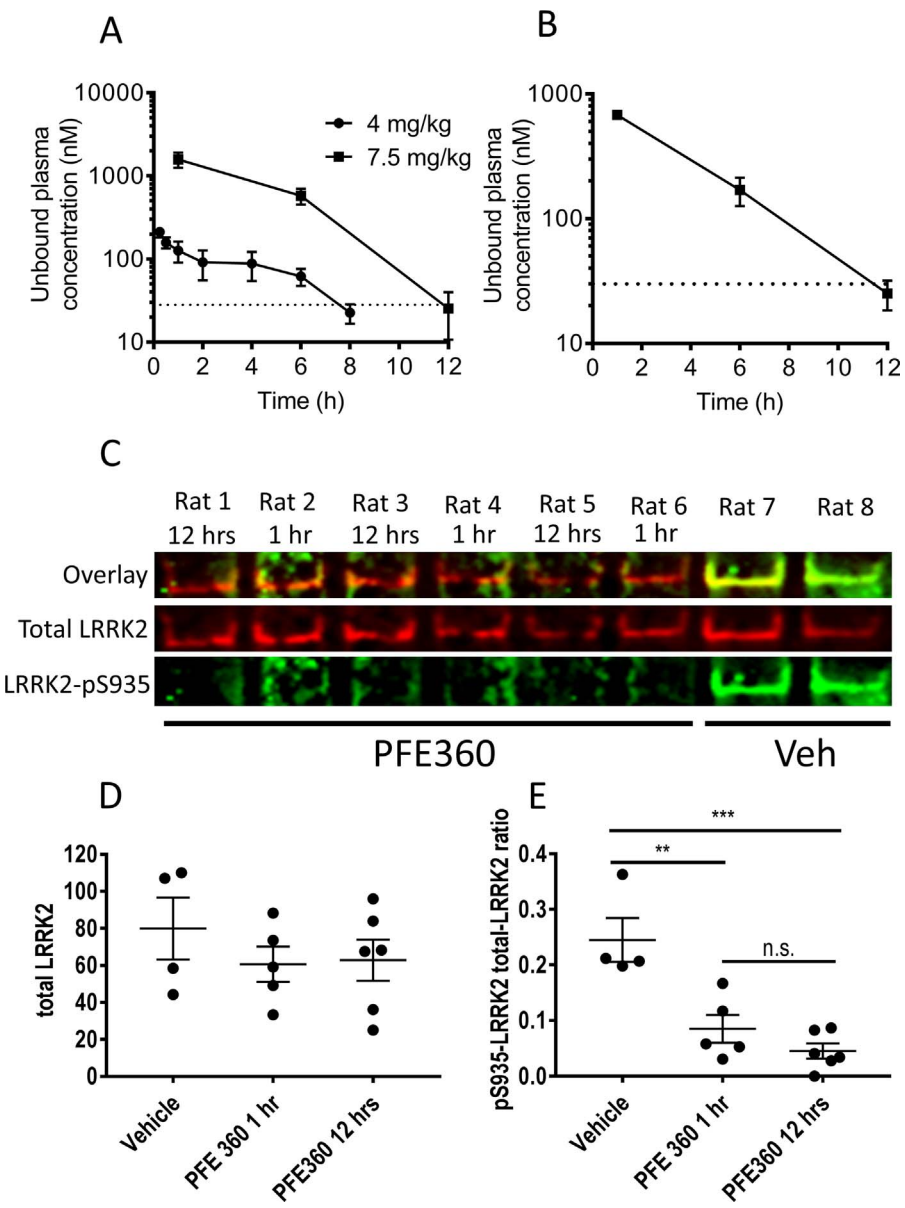

Fig. 1. Pharmacokinetic and pharmacodynamic properties of PFE-360. (A) Graphical presentation of the plasma pharmacokinetics of PFE-360 after a single oral dose of 4 mg/kg or 7.5 mg/kg. The dashed line represents the PFE-360 unbound plasma concentration ($10 \times IC_{50}$ (30 nM)) where total LRRK2 inhibition is expected to occur. Data are presented as mean ± SEM (4 mg/kg N = 3; 7.5 mg/kg 1, 3 and 6 h N = 3, 12 h N = 4). **(B)** Graphic presentation of unbound plasma concentrations of PFE-360 after multiple oral doses of 7.5 mg/kg PFE-360 BID. The dashed line represents the LRRK2 unbound plasma concentration ($10 \times IC_{50}$ (30 nM)) expected to result in full LRRK2 inhibition. Data are presented as mean ± SEM (1 h N = 5, 6 and 12 h N = 6) **(C)** Representative Western blot of total LRRK2 (red, top) and LRRK2-pSer935 (green, bottom) expression in kidney samples after 1–8 weeks of dosing with vehicle or PFE-360 at 7.5 mg/kg BID. **(D)** Graphical presentation of Western blot assessment of total LRRK2 expression in the kidneys after 1–8 weeks of dosing with 7.5 mg/kg PFE-360 at both 1 h and 12 h after dosing. Data are presented as mean ± SEM, the scatter plot represents the value of the individual animals. **(E)** Graphic presentation of the ratio of LRRK2-pSer935 to total-LRRK2 expression in the kidneys obtained using Western blot after 1–8 weeks of dosing with 7.5 mg/kg PFE-360 at both 1 h and 12 h after dosing. All data are shown as mean ± SEM, the scatter plot represents the value of the individual animals. Results of Tukey's multiple comparisons are shown on the figure. N.S.: non-significant, *:$0.05 > p > 0.01$, **:$0.01 > p > 0.001$ and ***:$p < 0.001$. (For interpretation of the references to colour in this figure legend, the reader is referred to the web version of this article.)

3.4. Kidney and lung findings after PFE-360 treatment for 10–12 weeks

The kidney weights were not significantly different between rats treated with vehicle or 7.5 mg/kg PFE-360 BID. Nor were any significant changes observed in lung weights in vehicle and PFE-360 treated groups (*t*-test; $p > 0.05$, Suppl. Table 1).

At the macroscopic examination, the kidneys of all PFE-360 treated rats exhibited a noticeable darkening like that described in LRRK2 ko rats (Fig. 2A). Microscopically, hyaline droplets were readily seen in the cytoplasm of the renal proximal cortical tubules of all PFE-360 treated animals in the HE stained sections. The Schmorl stained sections showed positive staining of the vast majority of tubular droplets in all PFE-360 treated rats (Fig. 2B–E). The kidneys were unstained with Perl's method (data not shown).

All vehicle treated rats showed weak positive Schmorl staining of small droplets in the cortical tubular cytoplasm. These droplets were not apparent in the HE stained kidney sections.

There were no other microscopic kidney findings.

The macroscopic and microscopic examination of the lung did not reveal any changes related to PFE-360 treatment.

3.5. Onset of kidney changes after PFE-360 treatment

The kidney morphology was evaluated after 1, 2, 4, 6 and 8 weeks of PFE-360 treatment at 7.5 mg/kg BID. Macroscopically, the group treated for 1 week displayed either no or very slight renal darkening when compared to vehicle treated animals, whereas all animals in the PFE-360 groups treated for 2 weeks and longer showed darkening of the kidneys (Suppl. Fig. 2).

At the histological examination, a progressive accumulation of cytoplasmic hyaline droplets was seen in the renal cortical tubules in the HE stained sections from all rats dosed with PFE-360 for 4. 6 and 8 weeks, but was not observed at the 1 and 2 week time-points (Table 1).

In the Schmorl stained sections, increased occurrence of positive droplets was detected in the cortical tubules after 2 weeks of PFE-360 treatment, and the frequency and staining intensity of these droplets increased progressively from 2 to 8 weeks of treatment (Table 1).

3.6. Reversibility of PFE-360 induced kidney changes

The kidneys were evaluated on day 2, 9, 16 and 30 after cessation of the 8 week treatment with PFE-360 at 4 or 7.5 mg/kg BID. On day 2

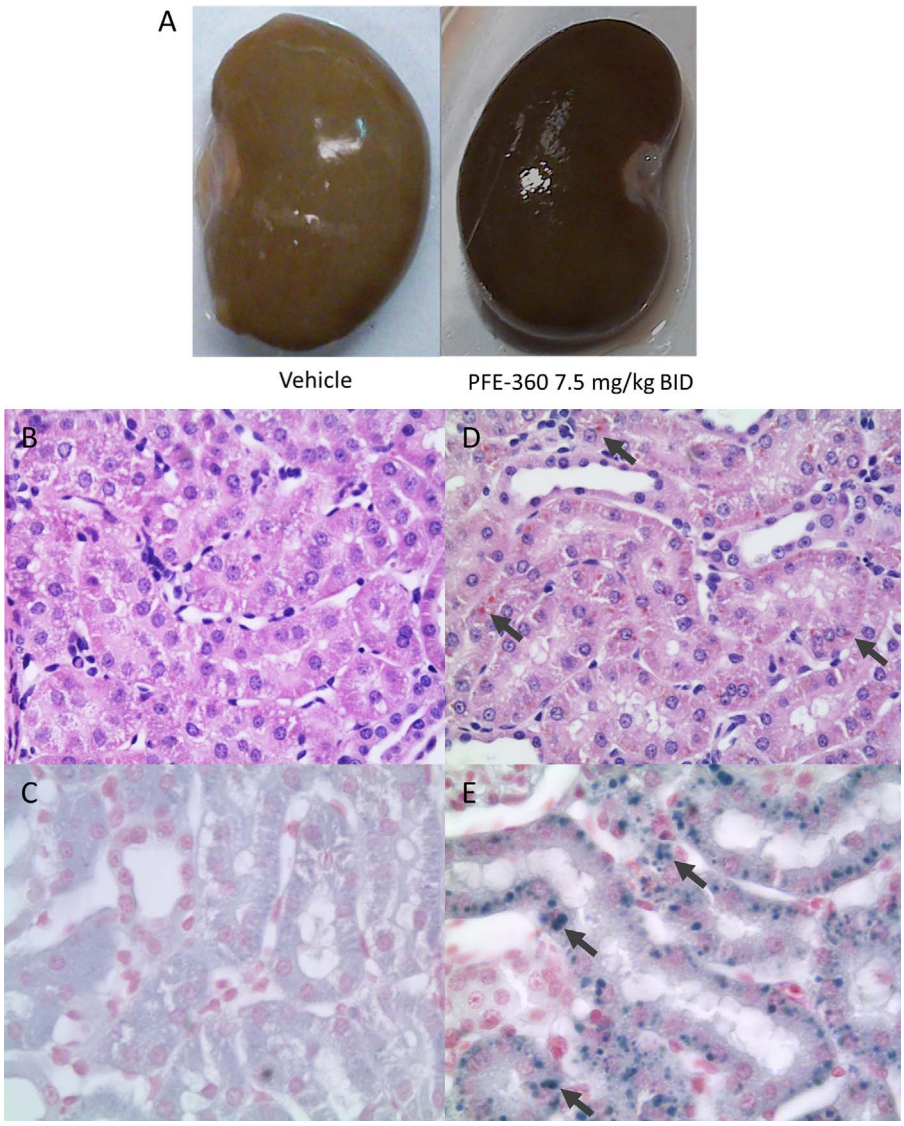

Fig. 2. Macroscopic and microscopic kidney changes after LRRK2 inhibition using PFE-360. (A) Macroscopic morphology of decapsulated kidneys after 10 weeks of treatment with vehicle or 7.5 mg/kg PFE-360 BID. The kidney is darkened after treatment with PFE-360. **(B + D)** H&E stained sections of kidney from a rat treated with vehicle (11 weeks) (B) and a rat treated with PFE-360 at 7.5 mg/kg (10 weeks) (D) BID (Obj. 40×). **(C + E)** Kidney sections stained with Schmorl's stain from a rat treated with vehicle (11 weeks) (C) or PFE-360 at 7.5 mg/kg (10 weeks) (D), BID (Obj. 63×). The arrows indicate hyaline droplets in the cytoplasm of the cortical tubuloepithelial cells in D, and the droplets staining positive by Schmorl's method in E, respectively.

Table 1
Summary of histopathological changes found in rat kidneys after 1. 2. 4. 6 and 8 weeks of treatment with PFE-360 at 7.5 mg/kg BID. Similar findings were made in all rats within the respective groups and were summarized as: −: not present; +−.+. ++. +++: increasing relative number, size, and/or staining intensity of a finding. NA: not assessed. Vehicle group: N = 4 (8 weeks of treatment); PFE-360 group: N = 2 (1. 2. 4. and 6 weeks of treatment) and N = 3 (8 weeks of treatment).

Weeks of PFE-360 dosing	Vehicle Hyaline droplets	Vehicle Schmorl positive droplets	PFE-360 7.5 mg/kg Hyaline droplets	PFE-360 7.5 mg/kg Schmorl positive droplets
1	NA	NA	–	+−
2	NA	NA	–	+
4	NA	NA	+	++
6	NA	NA	++	+++
8	–	+−	+++	+++

after cessation of treatment, the gross examination showed a darkening of the kidneys in all animals treated at 7.5 mg/kg BID. In the group treated with 4 mg/kg BID, the renal darkening was more variable between animals. On day 9 after cessation of treatment, there was a mild brown discolouration of the kidneys, with the most prominent change in the 7.5 mg/kg BID group. On day 16, the kidneys presented with a slight darkening in some treated animals, while being of normal colour in others. On day 30, there was no visual macroscopic difference in kidney colour among groups (Suppl. Fig. 3).

At the microscopic examination of the HE-stained kidney sections, cytoplasmic hyaline droplets were observed in the cortical tubules of most rats sacrificed on day 2 after cessation of the PFE-360 treatment, both at 4 mg/kg BID and 7.5 mg/kg BID (Table 2). The droplets stained positive by Schmorl's method. Hyaline droplets were detected in the HE stained sections at all subsequent time points after discontinuation of the PFE-360 treatment and showed no demonstrable change in appearance and number during the 30 day recovery period, whereas a clear progressive reduction in the occurrence and staining intensity of positive droplets was observed in the Schmorl stained sections in both PFE-360 treatment groups. By recovery day 30, the appearance of the renal tubules in the Schmorl stained sections was similar to that of vehicle-treated animals (Fig. 3 and Table 2).

4. Discussion

PFE-360 is a potent and selective LRRK2 inhibitor (Baptista et al., 2015). To achieve full peripheral LRRK2 inhibition, an estimated PFE-360 unbound plasma concentration of approximately 30 nM (~10 x IC_{50}) was targeted in our rat experiments. The single dose pharmacokinetic experiment indicated that this was achieved with a PFE-360

Table 2
Summary of histopathological changes found in rat kidneys 2. 9. 16 or 30 days after cessation of 8 weeks of treatment with PFE-360 at 4 mg/kg or 7.5 mg/kg BID. Similar findings were made in all rats within the respective groups and were summarized as: −: not present; + −.+. ++. +++: increasing relative number, size, and/or staining intensity of a finding. Vehicle group: N = 4 (Day 2. 9 and 30) and N = 2 (Day 16); PFE-360 at 4 mg/kg group: N = 2 per timepoint; PFE-360 at 7.5 mg/kg group: N = 4 per timepoint.

Recovery day (No. of day off treatment after 8 weeks of dosing)	Vehicle Hyaline droplets	Vehicle Schmorl positive droplets	PFE-360 4 mg/kg Hyaline droplets	PFE-360 4 mg/kg Schmorl positive droplets	PFE-360 7.5 mg/kg Hyaline droplets	PFE-360 7.5 mg/kg Schmorl positive droplets
2	–	+ −	+ +	+ + +	+ +	+ + +
9	–	+ −	+ +	+	+ +	+ +
16	–	+ −	+ +	+	+ +	+ +
30	–	+ −	+ +	+ −	+ +	+ −

dose of 7.5 mg/kg BID whereas a 4 mg/kg BID dose allowed for the LRRK2 inhibition in the peripheral organs to fall below full inhibition at trough levels.

Our study of the peripheral effects of pharmacological LRRK2 inhibition using PFE-360 revealed a progressive accumulation of hyaline droplets in the renal cortical tubules, which was not associated with histopathological evidence of renal tubular injury or changes in the blood and urine parameters, and thereby not suggestive of kidney toxicity or impaired kidney function. Schmorl positive cytoplasmic inclusions appeared histologically after 2 weeks of treatment and correlated with darkening of the kidneys, which was very prominent macroscopically. Hyaline droplets became detectable in HE stained sections after 4 weeks of treatment with the LRRK2 inhibitor. The morphological changes were partly reversible within a 30 day treatment-free period. A longer treatment-free period would be needed to conclude firmly on full reversibility of the kidney findings.

The changes in renal morphology observed at our histopathological examination are similar to those described in LRRK2 ko rats and LRRK2 ko and LRRK2 kinase dead mice (Baptista et al., 2013; Herzig et al., 2011). Baptista et al., 2013 stated that the histological appearance of the hyaline droplets in LRRK2 ko rats are very similar to those found in male rats with chemically-induced α2u-globulin nephropathy (Baptista et al., 2013; Hard and Khan, 2004). However, female rats have a very low expression of α2u-globulin and as a consequence they do not accumulate α2u-globulin in renal tubules (Ettlin et al., 2010). Hence, the hyaline droplets observed in this study in the kidney of female rats dosed with PFE-360 are considered unrelated to α2u-globulin.

Based on a number of histological staining methods, it has been suggested that LRRK2 ko rats and mice have a pathological accumulation of lipofuscin in the renal tubules (Baptista et al., 2013). In our study we saw an accumulation of droplets in the renal cortical tubules with a reductive ability in Schmorl's stain, which could be suggestive of lipofuscin (Lillie and Burtner, 1953). The prominent darkening of the kidneys seen macroscopically also suggests lipofuscin-like material, as lipofuscinosis of the kidneys is known to give rise to kidney darkening (Agerholm et al., 2009; Lund and Olsen, 1970). However, the increased positive Schmorl staining was reversible and the Schmorl-stained kidneys of PFE-360 treated animals were indistinguishable from those of vehicle-treated controls after 30 days off-treatment. This does not support that these elements are representing lipofuscin as there is evidence that lipofuscin is undegradable and unable to be exocytosed (Terman and Brunk, 1998a, 1998b). In addition, lipofuscin is normally visible in HE-stained tissue sections as a yellow-brown pigment, and such pigment was not observed in the renal tubular epithelium after the PFE-360 treatment.

Nevertheless, the composition of the Schmorl positive droplets might represent residual intracellular material such as oxidised lipid membrane and undegraded proteins with reductive properties in Schmorĺs test, which may have accumulated because of a deficit in the vesicular turnover. Rab GTPases function as key regulators of intracellular vesicular trafficking (Stenmark, 2009), and LRRK2 has recently been shown to phosphorylate a subset of Rab GTPases (Steger

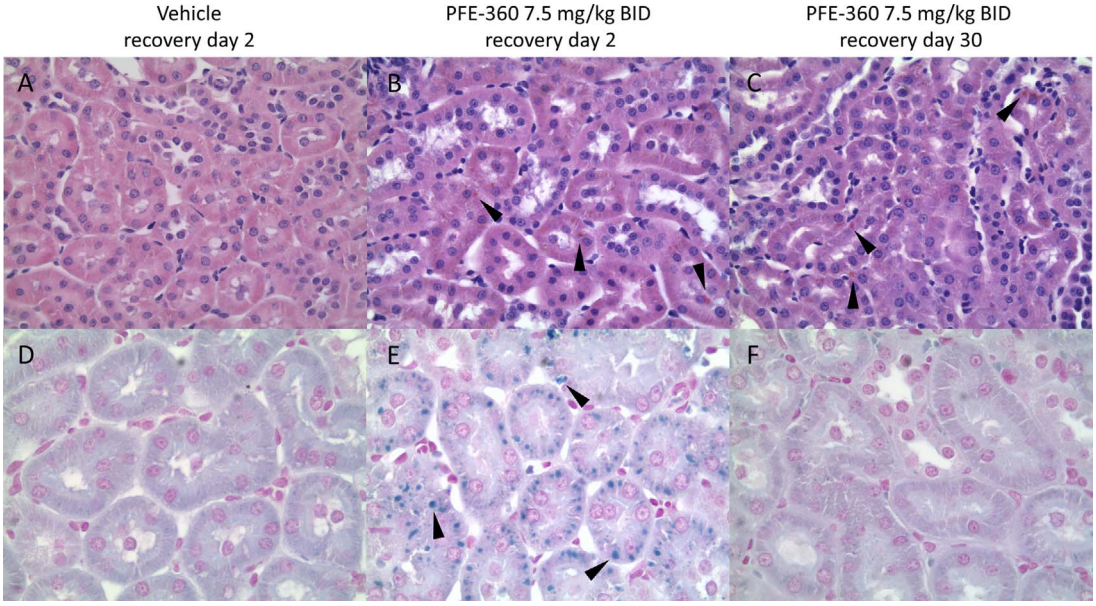

Fig. 3. Microscopic kidney changes after cessation of PFE-360 treatment. (A + B) H&E stained sections of kidney from rats treated with vehicle (A) or PFE-360 at 7.5 mg/kg (B) BID for 8 weeks and sampling of the kidneys 2 days after cessation of treatment (Obj. 40×). The PFE-360 treated animal shows hyaline droplets in the cytoplasm of the cortical tubuloepithelial cells (arrow heads). **(C)** H&E stained kidney section from rat treated for 8 weeks with 7.5 mg/kg PFE-360 BID and sampling of the kidneys 30 days after cessation of treatment. Arrow heads point at hyaline droplets similar to those found 2 days after discontinuation of treatment (Obj. 40×). **(D + E)** Schmorl stained kidney sections from rats treated with vehicle (D) or PFE-360 at 7.5 mg/kg (E) BID for 8 weeks and sampling of the kidneys 2 days after cessation of treatment (Obj. 63×). The PFE-360 treated animal shows positive staining of cytoplasmic droplets with Schmorl's method. **(F)** Schmorl stained kidney section from rat treated for 8 weeks with 7.5 mg/kg PFE-360 BID and sampling of the kidneys 30 days after cessation of treatment (Obj. 63×). The appearance of the renal tubules is similar to that of the vehicle treated animals.

et al., 2016) and to interact with the Rab7L1 protein. In accordance with these observations, LRRK2 ko animals have been reported to develop age-dependent accumulation of lysosomes and proteins in the proximal renal tubules (Baptista et al., 2013; Herzig et al., 2011; Tong et al., 2010). Further support for a common pathway involving LRRK2 and Rab7L1 comes from kidney changes that are reminiscent of the findings in LRRK2 ko animals that have been observed in Rab7L1 ko mice (Kuwahara et al., 2016; Steger et al., 2016).

In the study by Baptista et al., 2013, LRRK2 ko rats showed an accumulation of KIM-1 in the renal tubular epithelium, and it was recently reported that the LRRK2 substrate Rab5 is co-localised with KIM-1 in early and late endosomes of renal proximal tubular epithelium (Zhao et al., 2016), suggesting that the turn-over of KIM-1 is changed in LRRK2 ko rats due to changes in intravesicular trafficking. In this case, a decreased LRRK2 function may result in changes in KIM-1 turn-over, which might complicate the interpretation of KIM-1 as a marker of kidney injury in the safety assessment of LRRK2 inhibitors. Moreover, albeit measuring of urinary protein using Multistix® did not suggest changes in urinary protein content, assessment of urinary microalbumin could have been a useful additional marker of potential subclinical effects on renal function (Wiedmeyer and Royal, 2010). Nevertheless, we did not find changes in our study in any of the blood or urine parameters, or in the urinary kidney injury markers Kim-1, lipocalin or osteopontin. Hence, our study was not suggestive of changed kidney function or kidney injury after 10 to 12 weeks of treatment with PFE-360.

In LRRK2 ko rats, changes were observed in urine parameters (specific gravity, total urine volume, urine creatinine, total urine creatinine clearance, sodium/creatinine and chloride/creatinine), but these were more pronounced at 2 months of age compared to 8 months of age, suggesting adaptation (Baptista et al., 2013). In LRRK2 ko mice, proteinuria developed, but not until 18–22 months of age (Herzig et al., 2011), suggesting that impaired kidney function due to LRRK2 ablation takes a long time to develop. These functional alterations are likely more severe than those potentially induced by pharmacological inhibition. However, since we found morphological changes in the kidney similar to those observed in LRRK2 ko rats, our data supports that kidney function should be monitored in clinical studies with LRRK2 inhibitors.

In the present study, microscopic examination of the lung did not reveal any changes in the PFE-360-treated rats. In contrast, vacuolisation of type 2 pneumocytes has been reported in both monkeys and mice after pharmacological LRRK2 inhibition (Fell et al., 2015; Fuji et al., 2015). It is possible that the exposure of PFE-360 differs in the rat lung and kidneys, causing a lack of effect in the lung. Alternatively, PFE-360-induced lung changes in our study may have been too subtle to be detected by light microscopy. There is some support for this as accumulation of lamellar bodies was observed in type 2 pneumocytes in LRRK2 ko rats using electron microscopy, but not by light microscopy (Baptista et al., 2013).

5. In summary

Treatment of rats with PFE-360 at 7.5 mg/kg BID for up to 12 weeks resulted in full LRRK2 inhibition and induced morphological changes manifested by darkened kidneys and progressive accumulation of hyaline droplets in the renal tubular epithelium, without histopathological evidence of renal tubular injury or changes in blood and urine parameters that would be suggestive of kidney toxicity or impaired kidney function. Treatment with 4 mg/kg PFE-360 BID, which provided full LRRK2 inhibition for approximately 8 h per dosing, also resulted in macroscopical and histological changes in the kidneys, but to a lower extent than at 7.5 mg/kg PFE-360 BID. Morphological changes were detected in the kidneys after 2 weeks of treatment and were partially reversible within a 30 day treatment-free period. Our findings suggest that pharmacological LRRK2 inhibition may not have adverse consequences for kidney function. Additional studies using other LRRK2 inhibitor chemotypes and studies in higher species such as non-human primates are needed to fully substantiate this hypothesis.

Acknowledgements.

We thank Kirsten Christensen, Lise Maj Schrøder-Hansen, Marianne Kaarde and Mona Elisabeth Elster for excellent technical assistance. Furthermore, we thank the Danish Innovation Foundation for financial support.

Appendix A. Supplementary data

Supplementary data associated with this article can be found, in the online version, at https://doi.org/10.1016/j.tox.2018.01.003.

References

Agerholm, J.J.S., Christensen, K., Nielsen, S., Flagstad, P., 2009. Bovine renal lipofuscinosis: prevalence, genetics and impact on milk production and weight at slaughter in Danish cattle. Acta Vet. Scand. 51, 7.

Baptista, M.A.S., Dave, K.D., Frasier, M.A., Sherer, T.B., Greeley, M., Beck, M.J., Varsho, J.S., Parker, G.A., Moore, C., Churchill, M.J., Meshul, C.K., Fiske, B.K., 2013. Loss of leucine-rich repeat kinase 2 (LRRK2) in rats leads to progressive abnormal phenotypes in peripheral organs. PLoS One 8, e80705.

Baptista, M.A.S., Merchant, K., Bryce, D., Ellis, M., Estrada, A.A., Galatsis, P., Fell, M., Fuji, R.N., Kennedy, M.E., Hill, S., Hirst, W.D., Houle, C., Liu, X., Maddess, M., Markgraf, C., Mei, H., Steyn, S., Yin, Z., Yu, H., Fiske, B.K., Sherer, T.B., 2015. LRRK2 kinase inhibitors of different structural classes induce abnormal accumulation of lamellar bodies in type II pneumocytes in non-human primates but are reversible and without pulmonary functional consequences. Workflow and Study Design 94080.

Bundgaard, C., Sveigaard, C., Brennum, L.T., Stensbøl, T.B., 2012. Associating *in vitro* target binding and *in vivo* CNS occupancy of serotonin reuptake inhibitors in rats: the role of free drug concentrations. Xenobiotica 42, 256–265.

Daher, J.P.L., Abdelmotilib, H.A., Hu, X., Volpicelli-Daley, L.A., Moehle, M.S., Fraser, K.B., Needle, E., Chen, Y., Steyn, S.J., Galatsis, P., Hirst, W.D., West, A.B., 2015. Leucine-rich repeat kinase 2 (LRRK2) pharmacological inhibition abates α-Synuclein gene-induced neurodegeneration. J. Biol. Chem. 290, 19433–19444.

Ettlin, R.A., Kuroda, J., Plassmann, S., Hayashi, M., Prentice, D.E., 2010. Successful drug development despite adverse preclinical findings part 2: examples. J. Toxicol. Pathol. 23, 213–234.

Fell, M.J., Mirescu, C., Basu, K., Cheewatrakoolpong, B., DeMong, D.E., Ellis, J.M., Hyde, L.A., Lin, Y., Markgraf, C.G., Mei, H., Miller, M., Poulet, F.M., Scott, J.D., Smith, M.D., Yin, Z., Zhou, X., Parker, E.M., Kennedy, M.E., Morrow, J.A., 2015. MLi-2, a potent, selective, and centrally active compound for exploring the therapeutic potential and safety of LRRK2 kinase inhibition. J. Pharmacol. Exp. Ther. 355, 397–409.

Fuji, R.N., Flagella, M., Baca, M., Baptista, M.A.S., Brodbeck, J., Chan, B.K., Fiske, B.K., Honigberg, L., Jubb, A.M., Katavolos, P., Lee, D.W., Lewin-Koh, S.-C., Lin, T., Liu, X., Liu, S., Lyssikatos, J.P., O'Mahony, J., Reichelt, M., Roose-Girma, M., Sheng, Z., Sherer, T.B., Smith, A., Solon, M., Sweeney, Z.K., Tarrant, J., Urkowitz, A., Warming, S., Yaylaoglu, M., Zhang, S., Zhu, H., Estrada, A.A., Watts, R.J., 2015. Effect of selective LRRK2 kinase inhibition on nonhuman primate lung. Sci. Transl. Med. 7, 273ra15.

Hard, G.C., Khan, K.N., 2004. A contemporary overview of chronic progressive nephropathy in the laboratory rat, and its significance for human risk assessment. Toxicol. Pathol. 32.

Herzig, M.C., Kolly, C., Persohn, E., Theil, D., Schweizer, T., Hafner, T., Stemmelen, C., Troxler, T.J., Schmid, P., Danner, S., Schnell, C.R., Mueller, M., Kinzel, B., Grevot, A., Bolognani, F., Stirn, M., Kuhn, R.R., Kaupmann, K., van der Putten, P.H., Rovelli, G., Shimshek, D.R., 2011. LRRK2 protein levels are determined by kinase function and are crucial for kidney and lung homeostasis in mice. Hum. Mol. Genet. 20, 4209–4223.

Kuwahara, T., Inoue, K., D'Agati, V.D., Fujimoto, T., Eguchi, T., Saha, S., Wolozin, B., Iwatsubo, T., Abeliovich, A., 2016. LRRK2 and RAB7L1 coordinately regulate axonal morphology and lysosome integrity in diverse cellular contexts. Sci. Rep. 6, 29945.

Lillie, R.D., Burtner, H.J., 1953. The ferric ferricyanide reduction test in histochemistry. J. Histochem. Cytochem. 1, 87–92.

Luna, L., 1968. Manual of Histologic Staining Methods of the Armed Forces Institute of Pathology, 3rd ed. Blakiston Division McGraw-Hill, New York.

Lund, T., Olsen, S., 1970. Idiopathic renal lipofuscinosis. Acta Pathol. Microbiol. Scand. Sect. A Pathol. 78A, 414–420.

Reynolds, A., Doggett, E.A., Riddle, S.M., Lebakken, C.S., Nichols, R.J., 2014. LRRK2 kinase activity and biology are not uniformly predicted by its autophosphorylation and cellular phosphorylation site status. Front. Mol. Neurosci. 7, 54.

Steger, M., Tonelli, F., Ito, G., Davies, P., Trost, M., Vetter, M., Wachter, S., Lorentzen, E., Duddy, G., Wilson, S., Baptista, M.A., Fiske, B.K., Fell, M.J., Morrow, J.A., Reith, A.D., Alessi, D.R., Mann, M., 2016. Phosphoproteomics reveals that Parkinson's disease kinase LRRK2 regulates a subset of Rab GTPases. Elife 5.

Stenmark, H., 2009. Rab GTPases as coordinators of vesicle traffic. Nat. Rev. Mol. Cell Biol. 10, 513–525.

Terman, A., Brunk, U.T., 1998a. Ceroid/lipofuscin formation in cultured human fibroblasts: the role of oxidative stress and lysosomal proteolysis. Mech. Ageing Dev. 104, 277–291.
Terman, A., Brunk, U.T., 1998b. On the degradability and exocytosis of ceroid/lipofuscin in cultured rat cardiac myocytes. Mech. Ageing Dev. 100, 145–156.
Tong, Y., Yamaguchi, H., Giaime, E., Boyle, S., Kopan, R., Kelleher, R.J., Shen, J., 2010. Loss of leucine-rich repeat kinase 2 causes impairment of protein degradation pathways, accumulation of alpha-synuclein, and apoptotic cell death in aged mice. Proc. Natl. Acad. Sci. U. S. A. 107, 9879–9884.
Trainor, G.L., 2007. The importance of plasma protein binding in drug discovery. Expert Opin. Drug Discov. 2, 51–64.
Wiedmeyer, C.E., Royal, A.B., 2010. Urinary biomarkers for monitoring disease progression in the Han:SPRD-cy rat model of autosomal-dominant polycystic kidney disease. Comp. Med. 60, 448–454.
Zhao, X., Jiang, C., Olufade, R., Liu, D., Emmett, N., 2016. Kidney injury molecule-1 enhances endocytosis of albumin in renal proximal tubular cells. J. Cell. Physiol. 231, 896–907.
Zimprich, A., Biskup, S., Leitner, P., Lichtner, P., Farrer, M., Lincoln, S., Kachergus, J., Hulihan, M., Uitti, R.J., Calne, D.B., Stoessl, A.J., Pfeiffer, R.F., Patenge, N., Carbajal, I.C., Vieregge, P., Asmus, F., Müller-Myhsok, B., Dickson, D.W., Meitinger, T., Strom, T.M., Wszolek, Z.K., Gasser, T., 2004a. Mutations in LRRK2 cause autosomal-Dominant parkinsonism with pleomorphic pathology. Neuron 44, 601–607.
Zimprich, A., Müller-Myhsok, B., Farrer, M., Leitner, P., Sharma, M., Hulihan, M., Lockhart, P., Strongosky, A., Kachergus, J., Calne, D.B., Stoessl, J., Uitti, R.J., Pfeiffer, R.F., Trenkwalder, C., Homann, N., Ott, E., Wenzel, K., Asmus, F., Hardy, J., Wszolek, Z., Gasser, T., 2004b. The PARK8 locus in autosomal dominant parkinsonism: confirmation of linkage and further delineation of the disease-containing interval. Am. J. Hum. Genet. 74, 11–19.